PNAS
www.pnas.org

Supplementary Information for

Crystal structure of heme A synthase from *Bacillus subtilis*

Satomi Niwa, Kazuki Takeda, Masayuki Kosugi, Erika Tsutsumi, Tatsushi Mogi, and Kunio Miki

Kunio Miki
Email: miki@kuchem.kyoto-u.ac.jp

This PDF file includes:

Figs. S1 to S7
Tables S1 to S3
Captions for data S1

Other supplementary materials for this manuscript include the following:

Data S1

www.pnas.org/cgi/doi/10.1073/pnas.1813346115

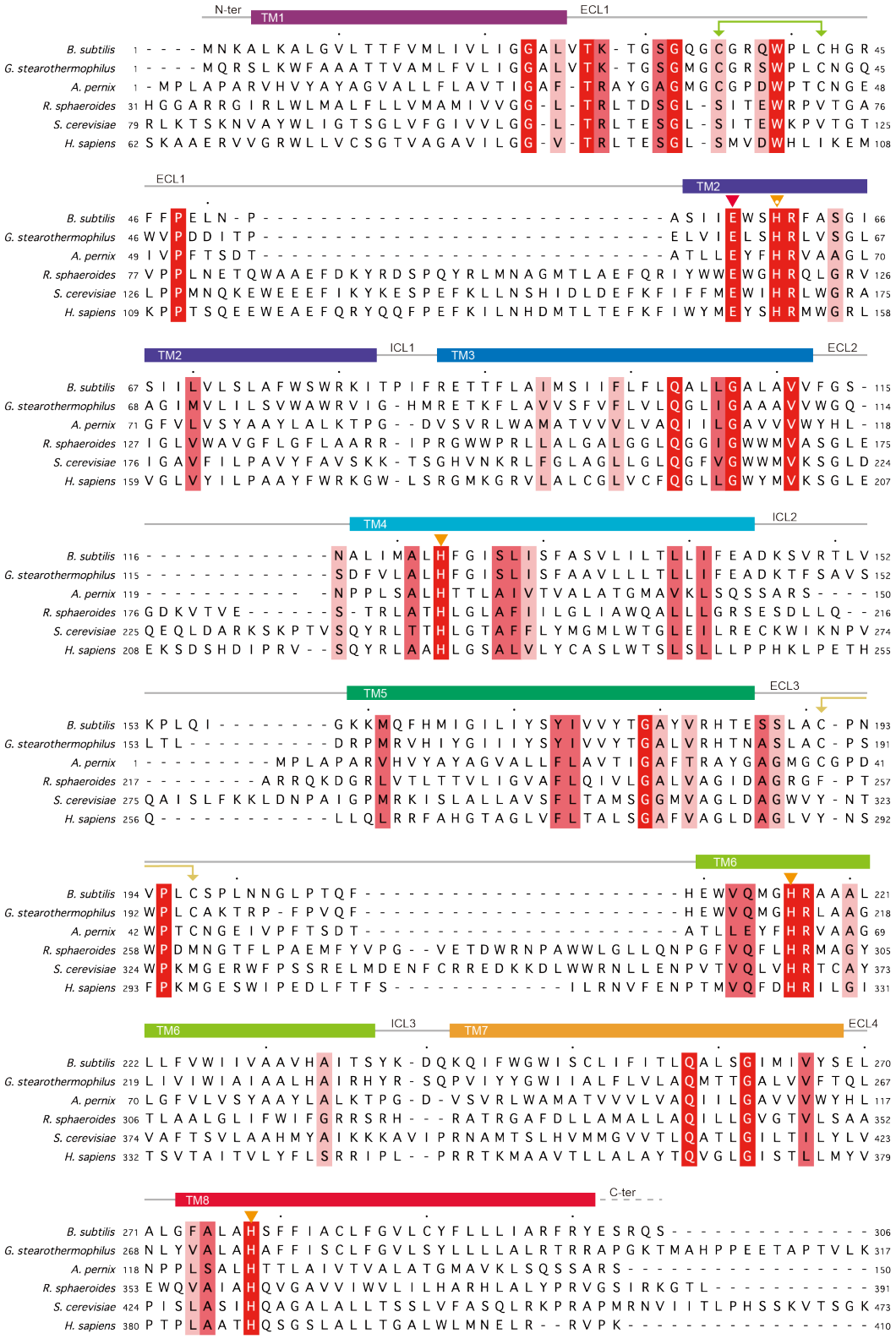
N-ter
TM1
ECL1
B. subtilis 1 - - - - MNKALKALGVLTTFVMLIVLIGGALVTK-TGSGQGCGRQWPLCHGR 45
G. stearothermophilus 1 - - - - MQRSLKWFAAATTVAMLFVLIGGALVTK-TGSGMGCGRSWPLCNGQ 45
A. pernix 1 - MPLAPARVHVYAYAGVALLFLAVTIGAF-TRAYGAGMGCGPDWPTCNGE 48
R. sphaeroides 31 HGGARRGIRLWLMALFLLVMAMIVVGG-L-TRLTDSGL-SITEWRPVTGA 76
S. cerevisiae 79 RLKTSKNVAYWLIGTSGLVFGIVVLGG-L-TRLTESGL-SITEWKPVTGT 125
H. sapiens 62 SKAAERVVGRWLLVCSGTVAGAVILGG-V-TRLTESGL-SMVDWHLIKEM 108
ECL1
TM2
B. subtilis 46 FFPELN-P - ASIIEWSHRFASGI 66
G. stearothermophilus 46 WVPDDITP - ELVIELSHRLVSGL 67
A. pernix 49 IVPFTSDT - ATLLEYFHRVAAGL 70
R. sphaeroides 77 VPPLNETQWAAEFDKYRDSPQYRLMNAGMTLAEFQRIYWWEWGHRQLGRV 126
S. cerevisiae 126 LPPMNQKEWEEEFIKYKESPEFKLLNSHIDLDEFKFIFFMEWIHRLWGRA 175
H. sapiens 109 KPPTSQEEWEAEFQRYQQFPEFKILNHDMTLTEFKFIWYMEYSHRMWGRL 158
TM2
ICL1
TM3
ECL2
B. subtilis 67 SIILVLSLAFWSWRKITPIFRETTFLAIMSIIFLFLQALLGALAVFGS- 115
G. stearothermophilus 68 AGIMVLILSVWAWRVIG-HMRETKFLAVVSFVFLVLQGLIGAAAVVWGQ- 114
A. pernix 71 GFVLVSYAAYLALKTPG--DVSVRLWAMATVVVLVAQIILGAVVVWYHL- 118
R. sphaeroides 127 IGLVWAVGFLGFLAARR-IPRGWWPRLLALGALGGLQGGIGWWMVASGLE 175
S. cerevisiae 176 IGAVFILPAVYFAVSKK-TSGHVNKRLFGLAGLLGLQGFVGWWMVKSGLD 224
H. sapiens 159 VGLVYILPAAYFWRKGW-LSRGMKGRVLALCGLVCFQGLLGWYMVKSGLE 207
TM4
ICL2
B. subtilis 116 - - - - - - - - - - - - - NALIMALHFGISLISFASVLILTLLIFEADKSVRTLV 152
G. stearothermophilus 115 - - - - - - - - - - - - - SDFVLALHFGISLISFAAVLLLTLLIFEADKTFSAVS 152
A. pernix 119 - - - - - - - - - - - - - NPPLSALHTTLAIVTVALATGMAVKLSQSSSARS- - - - 150
R. sphaeroides 176 GDKVTVE- - - - - - S-TRLATHLGLAFIILGLIAWQALLLGRSESDLLQ- - 216
S. cerevisiae 225 QEQLDARKSKPTVSQYRLTTHLGTAFFLYMGMLWTGLEILRECKWIKNPV 274
H. sapiens 208 EKSDSHDIPRV--SQYRLAAHLGSALVLYCASLWTSLSLLLPPHKLPETH 255
TM5
ECL3
B. subtilis 153 KPLQI - - - - - - - - GKKMQFHMIGILIYSYIVVYTGAYVRHTESSLAC-PN 193
G. stearothermophilus 153 LTL - - - - - - - - - - DRPMRVHIYGIIIYSYIVVYTGALVRHTNASLAC-PS 191
A. pernix 1 - - - - - - - - - - MPLAPARVHVYAYAGVALLFLAVTIGAFTRAYGAGMGCGPD 41
R. sphaeroides 217 - - - - - - - - - ARRQKDGRLVTLTTVLIGVAFLQIVLGALVAGIDAGRGF-PT 257
S. cerevisiae 275 QAISLFKKLDNPAIGPMRKISLALLAVSFLTAMSGGMVAGLDAGWVY-NT 323
H. sapiens 256 Q - - - - - - - - - - - - - LLQLRRFAHGTAGLVFLTALSGAFVAGLDAGLVY-NS 292
TM6
B. subtilis 194 VPLCSPLNNGLPTQF - HEWVQMGHRAAAL 221
G. stearothermophilus 192 WPLCAKTRP-FPVQF - HEWVQMGHRLAAG 218
A. pernix 42 WPTCNGEIVPFTSDT - ATLLEYFHRVAAG 69
R. sphaeroides 258 WPDMNGTFLPAEMFYVPG--VETDWRNPAWWLGLLQNPGFVQFLHRMAGY 305
S. cerevisiae 324 WPKMGERWFPSSRELMDENFCRREDKKDLWWRNLLENPVTVQLVHRTCAY 373
H. sapiens 293 FPKMGESWIPEDLFTFS - - - - - - - - - - - - - ILRNVFENPTMVQFDHRILGI 331
TM6
ICL3
TM7
ECL4
B. subtilis 222 LLFVWIIVAAVHAITSYK-DQKQIFWGWISCLIFITLQALSGIMIVYSEL 270
G. stearothermophilus 219 LIVIWIAIAALHAIRHYR-SQPVIYYGWIIALFLVLAQMTTGALVVFTQL 267
A. pernix 70 LGFVLVSYAAYLALKTPG-D-VSVRLWAMATVVVLVAQIILGAVVVWYHL 117
R. sphaeroides 306 TLAALGLIFWIFGRRSRH- - - RATRGAFDLLAMALLAQILLGVGTVLSAA 352
S. cerevisiae 374 VAFTSVLAAHMYAIKKKAVIPRNAMTSLHVMMGVVTLQATLGILTILYLV 423
H. sapiens 332 TSVTAITVLYFLSRRIPL--PRRTKMAAVTLLALAYTQVGLGISTLLMYV 379
TM8
C-ter
B. subtilis 271 ALGFALAHSFFIACLFGVLCYFLLLIARFRYESRQS - - - - - - - - - - - - - - 306
G. stearothermophilus 268 NLYVALAHAFFISCLFGVLSYLLLLALRTRRAPGKTMAHPPEETAPTVLK 317
A. pernix 118 NPPLSALHTTLAIVTVALATGMAVKLSQSSSARS- - - - - - - - - - - - - - 150
R. sphaeroides 353 EWQVAIAHQVGAVVIWVLILHARHLALYPRVGSIRKGTL- - - - - - - - - - - - 391
S. cerevisiae 424 PISLASIHQAGALALLTSSLVFASQLRKPRAPMRNVIITLPHSSKVTSGK 473
H. sapiens 380 PTPLAATHQSGSLALLTGALWLMNELR--RVPK - - - - - - - - - - - - - - - 410

Fig. S1. Sequence alignment of HAS. Fully, highly and relatively conserved residues are shaded in red, light red and pale red, respectively. HASs from *B. subtilis*, *Geobacillus stearothermophilus* and *Aeropyrum pernix* are classified into type-1 HAS, and HASs from *Rhodobacter sphaeroides*, *Saccharomyces cerevisiae* and *Homo sapiens* are classified into type-2 HAS. Secondary structural elements of HAS from *B. subtilis* are indicated above the sequence alignment. The conserved glutamate residue and histidine residues are labeled with red and orange triangles, respectively. The disulfide bridges in ECL1 (conserved in only type-1 HAS) and ECL3 are indicated with green and yellow arrows.

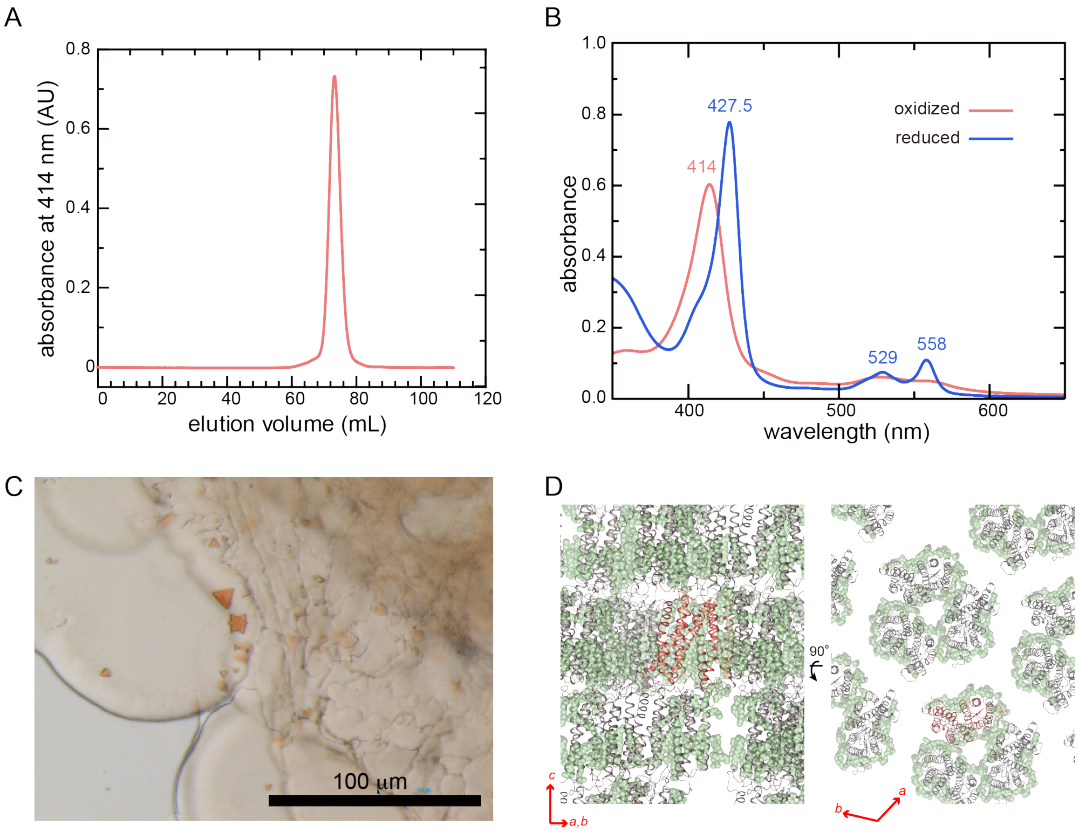

Fig. S2. Purification and crystallization of HAS. (*A*) Elution profile of the BsHAS during the last size exclusion chromatography step. (*B*) The absorption spectrum for the air-oxidized, as prepared BsHAS (pink) and ascorbate-reduced BsHAS (blue). (*C*) Crystals of BsHAS obtained in lipidic cubic phase. (*D*) Crystal packing viewed along the *a* (left) and *c* (right) axes. The monoolein molecules are shown as green spheres.

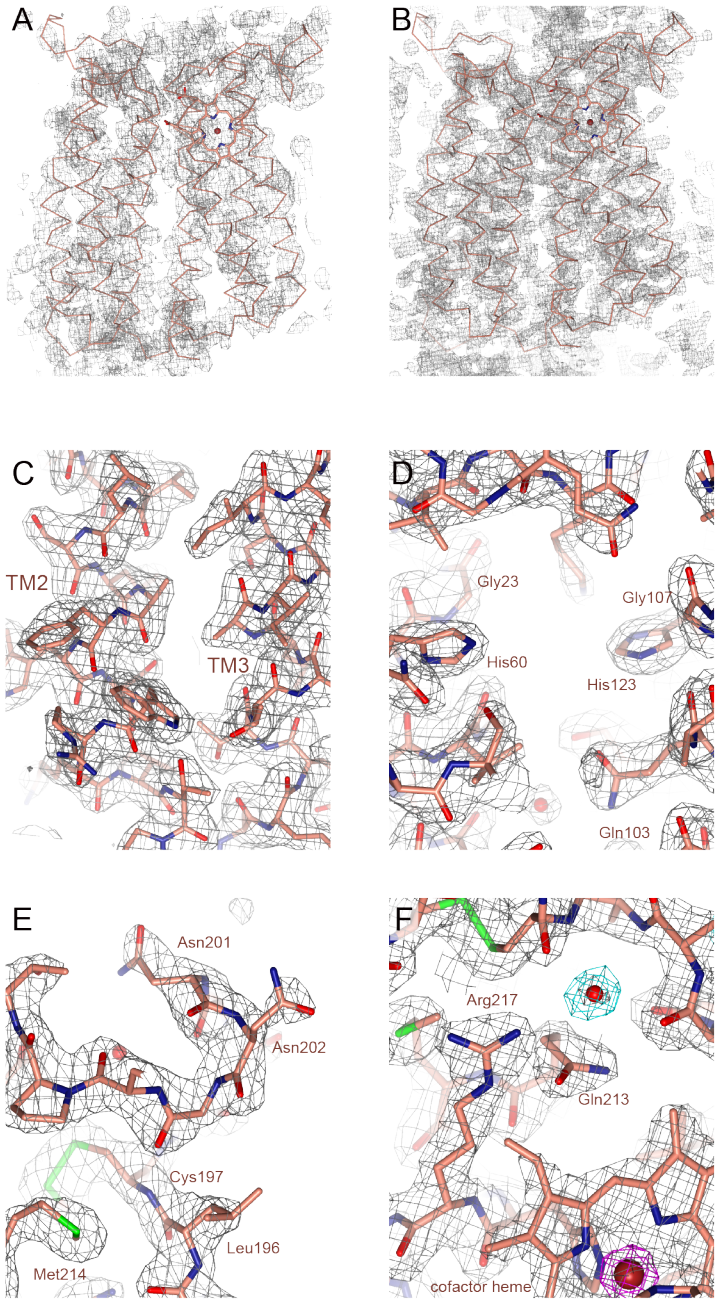

Fig. S3. Electron density maps for BsHAS. (*A*) The initial electron density maps obtained from MIRAS (20–3.5 Å; gray mesh, 1.0σ) superimposed onto a Cα model. (*B*)–(*F*), The final $2mF_{obs}-DF_{calc}$ electron density map (30–2.2 Å; gray mesh, 1.0σ). Close-up views of TM2 and TM3 (*C*), the substrate-heme-binding site (*D*), ECL3 (*E*) and cofactor-heme-binding site (*F*) are also shown. In panel (*F*), the additional final $2mF_{obs}-DF_{calc}$ electron density map (magenta mesh, 8.0σ) and the omit map for a water molecule is also shown (cyan mesh, 4.0σ).

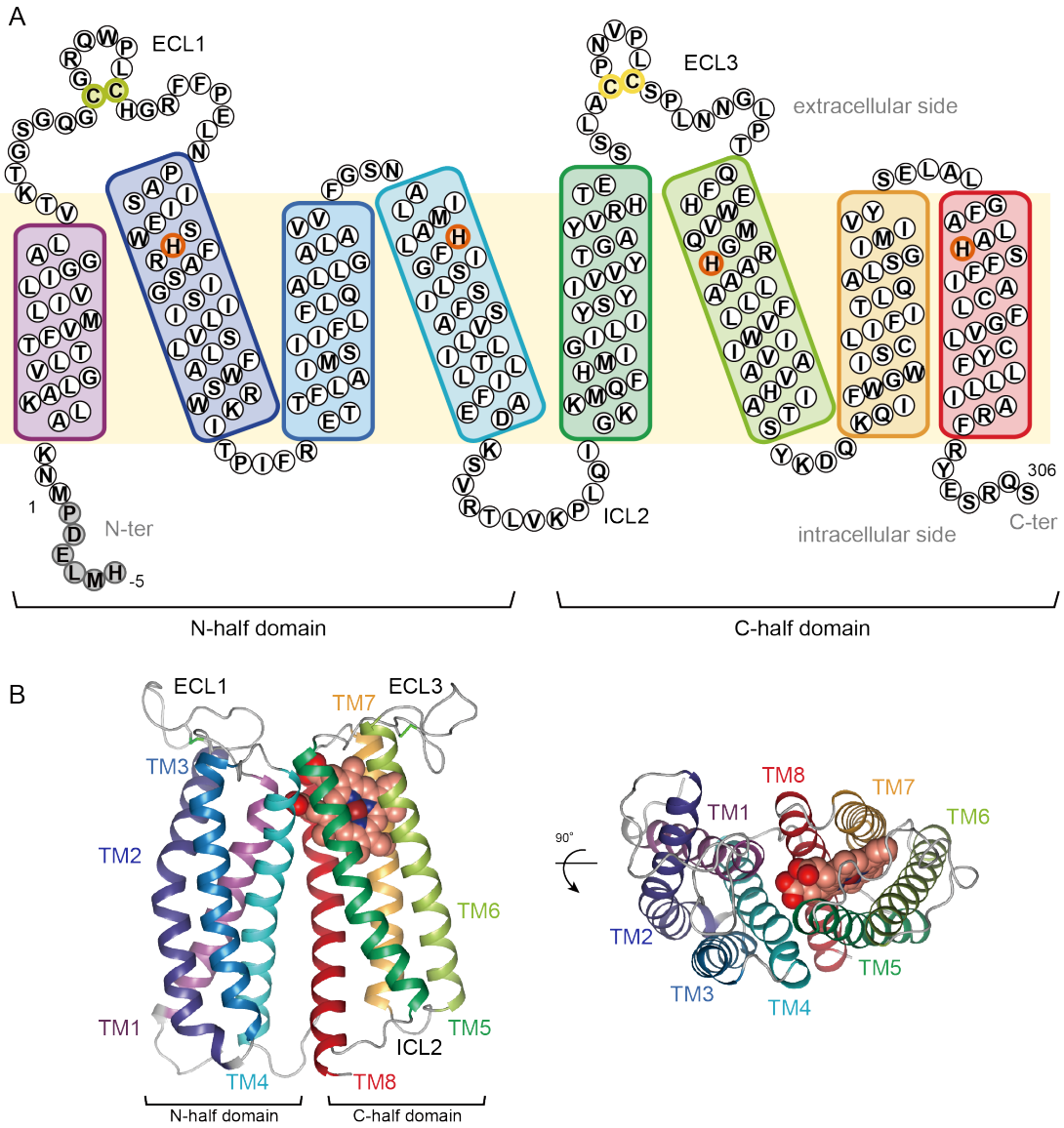

Fig. S4. (*A*) Schematic representation of HAS from the *B. subtilis* construct used in this study. The conserved histidine residues serving as heme axial ligands, cysteine residues forming disulfide bridges and a part of the thrombin cleavage site are colored in orange, green/yellow, and gray, respectively. The α-helical structure of the transmembrane region is assigned from the crystal structure. (*B*) The crystal structure of BsHAS as viewed from within the membrane and the extracellular side.

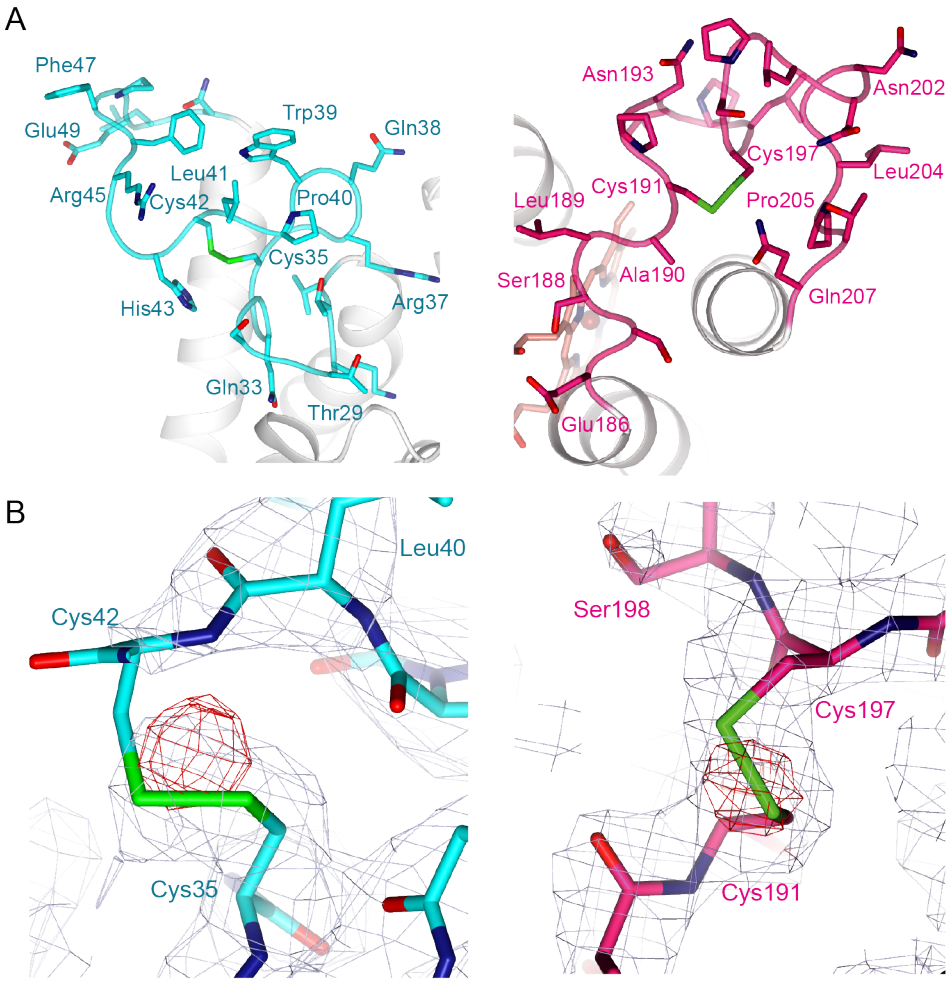

Fig. S5. Structure of ECL1 and ECL3. (*A*) Structure of the extracellular loop region, ECL1 (left) and ECL3 (right). (*B*) Disulfide bridges of ECL1 and ECL3. Anomalous difference Fourier maps calculated with the data collected at 1.75 Å wavelength are indicated by red mesh (3.0σ). The final 2mF_{obs}−DF_{calc} electron density map for these data is also shown (1.0σ, gray mesh).

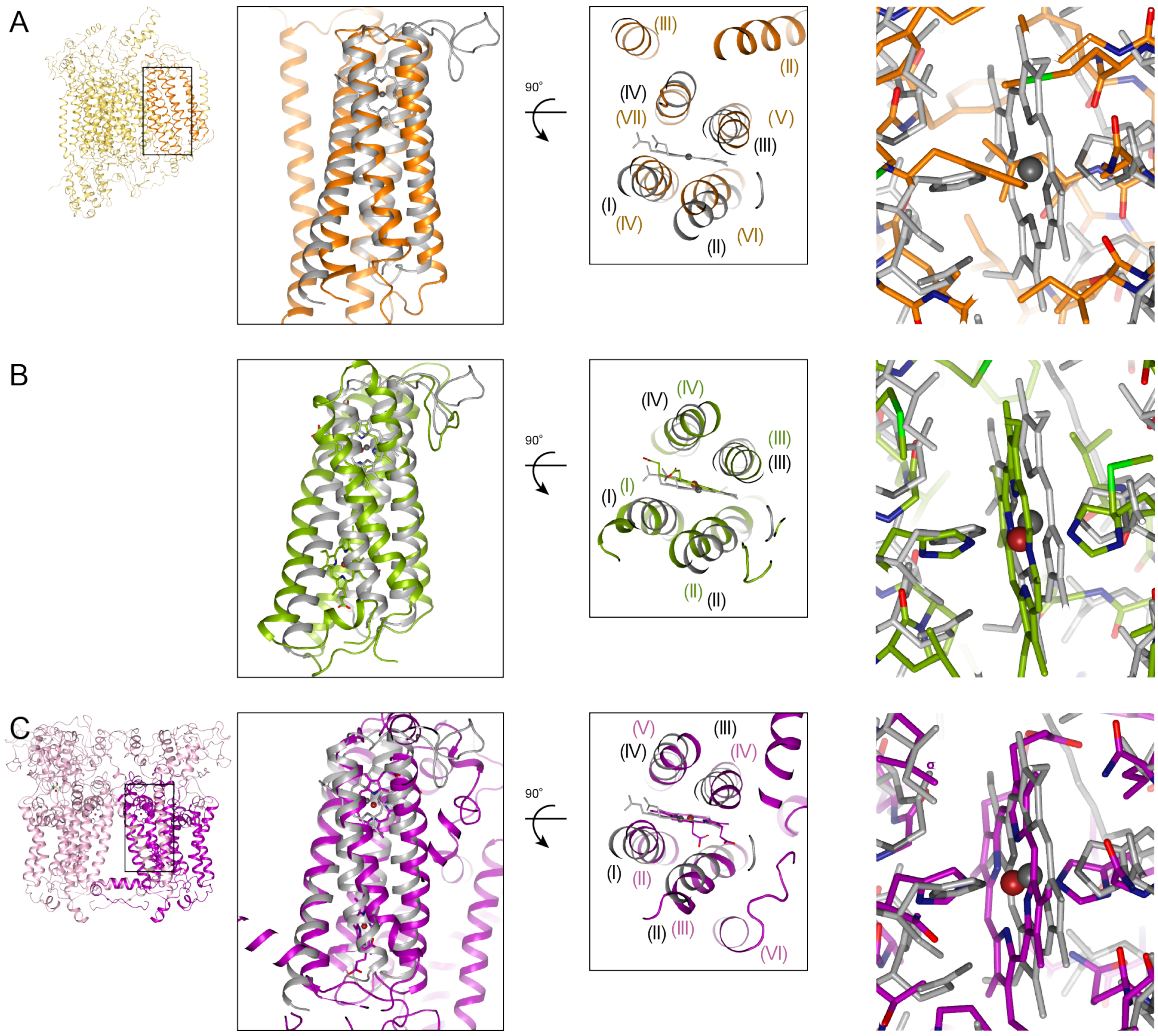

Fig. S6. Superimposition between C-half domain of BsHAS and the structurally similar proteins indicated by Dali. Main chains of the similar structures are shown as ribbon drawing (left). The C-half domain of BsHAS is shown in gray as a reference. In addition, close-up views of cofactor-heme-binding site are shown (right). (*A*) Subunit III in cytochrome *c* oxidase from bovine (PDB-ID: 1OCC, chain C). (*B*) Superoxide oxidase from *E. coli* (PDB-ID: 5OC0). (*C*) Cytochrome *b* in cytochrome bc_1 complex from *R. sphaeroides* (PDB-ID: 5KKZ, chain A).

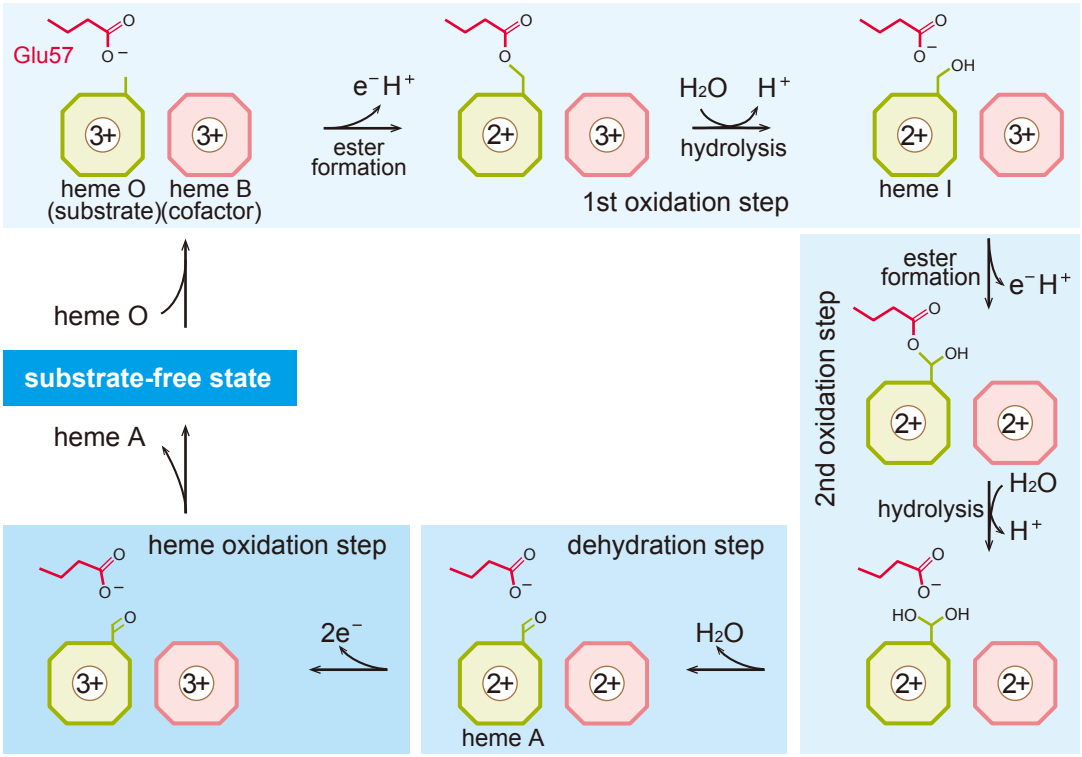

Fig. S7. Proposed reaction mechanism for the formylation reaction of heme A synthesis. Proposed reaction mechanism for the formylation reaction of heme A synthesis. This reaction scheme consists of four steps: two steps of single-electron oxidation, followed by dehydration, and the final heme oxidation. In the first 8-substituent oxidation step, heme O yields a heme radical, which generates an ester cross-link of the C-8 methyl group of heme O with the carboxylate group of Glu57. Following hydrolysis of the ester cross-link, a heme I is generated. Then the second single-electron oxidation step takes place in a manner similar to the first step and generates a geminal diol. Subsequently, spontaneous dehydration at the 8-substituant group yields heme A. In the final heme oxidation step, both heme A and B are reoxidized by the electron acceptor.

Table S1. Properties of constructed variants of overproduced BsHAS.

variant	expression host	types of heme	reference
wild type	*B. subtilis*	B, (A)	16
wild type	*E. coli*	B, (O, O_X)	10
W39A	*E. coli*	B, O, (O_X)	10
C35A	*B. subtilis*	B, O, (II, A)	17
C42A	*B. subtilis*	B, O, (II)	17
E57A	*E. coli*	B, O	10
E57Q	*E. coli*	B, O	10
H60L	*B. subtilis*	B, O	16
H60M	*B. subtilis*	B, (A)	16
H60A	*E. coli*	B, (O)	10
H60Q	*E. coli*	B, (O)	10
R61A	*E. coli*	B, (O)	10
R61Q	*E. coli*	B, (O)	10
Q103A	*E. coli*	B, O_X, (O)	10
H123L	*B. subtilis*	B, O	16
H123M	*B. subtilis*	B, O	16
H123A	*E. coli*	B, (O)	10
H123Q	*E. coli*	B, (O)	10
C191A	*B. subtilis*	N.D.	17
C197A	*B. subtilis*	N.D.	17
H216L	*B. subtilis*	not expressed	16
H216M	*B. subtilis*	B, O, I	16
H216A	*E. coli*	B, O, O_X, O_Y	10
H216Q	*E. coli*	B, O, O_X	10
R217A	*E. coli*	B, O, O_X	10
R217Q	*E. coli*	B, O_X, (O)	10
Q258A	*E. coli*	B, O_X, (O)	10
H278L	*B. subtilis*	(B, A)	16
H278M	*B. subtilis*	(B, A)	16
H278A	*E. coli*	B, (O, O_Y)	10
H278Q	*E. coli*	B, O, O_X	10
C35A/C42A	*B. subtilis*	N.D.	17
C35A/C42A	*E. coli*	B, O	10
C35A/C191A	*B. subtilis*	N.D.	17
C35A/C197A	*B. subtilis*	N.D.	17
C35A/C42A/C191A	*B. subtilis*	N.D.	17
C35A/C42A/C191A/C197A	*B. subtilis*	B, O, II	17
H60A/H123A	*E. coli*	B, (O, O_X)	10
H60Q/H123Q	*E. coli*	B, O_X, (O)	10
C191A/C197A	*B. subtilis*	B, A, II, (O)	17
C191A/C197A	*E. coli*	B, O, O_Y	10

Traces of heme are indicated with brackets.
O_X, O_Y: 8-hydroxymethyl derivatives of heme O.
I: 8-alcohol derivative of heme O (heme I).
II: 8-carboxylate derivative of heme O (heme II).
N.D.: Not determined.

Table S2. Data collection and phasing statistics.

	Native	S-anomalous	Fe-anomalous	Hg-derivative	Pt-derivative
Data collection					
Wavelength (Å)	1.00	1.75	1.74	1.00	1.00
Space group	*H*3	*H*3	*H*3	*H*3	*H*3
Cell dimensions					
a=*b* (Å)	90.47	90.53	91.01	91.00	89.93
c (Å)	147.32	147.23	148.18	148.59	148.20
Resolution (Å)	50–2.20	50–3.00	50–3.50	50–3.38	50–4.00
	(2.32–2.20)*	(3.11–3.00)	(3.56–3.50)	(3.59–3.38)	(4.14–4.00)
No. of reflections	119,694	178,985	57,778	66,991	38,991
Unique reflections	22,834	8,987	5,737	6,387	3,797
Completeness (%)	99.9 (99.7)	100.0 (100.0)	100.0 (100.0)	99.6 (98.0)	100.0 (100.0)
Redundancy	5.2 (5.1)	19.9 (19.7)	10.1 (10.4)	10.5 (9.7)	10.2 (10.3)
R_{sym} (%)†	12.7 (123.0)	27.7 (113.0)	15.7 (85.6)	22.7 (110.3)	24.2 (106.7)
$I/\sigma(I)$	8.02 (1.20)	11.5 (2.3)	11.9 (2.3)	8.58 (2.02)	8.9 (1.92)
CC(1/2) (%)	99.7 (49.4)	- (82.4)	- (84.3)	99.6 (82.5)	- (85.8)
Twin fraction (%)	3	3	3	4	6
Phasing (MIRAS)					
No.of heavy atom sites			1 (Fe in heme)	3	2
Isomorphous phasing power			-	1.78	1.60
Anomalous phasing power			0.55	0.71	0.48
FOM‡ (SOLVE, 20–4.2 Å)			0.63		
FOM (RESOLVE, 20–3.5 Å)			0.74		

* Values in parentheses are for the highest-resolution shell.

† $R_{sym} = \Sigma_{hkl}\Sigma_i| I_{hkl,I} - \langle I_{hkl}\rangle|/\Sigma_{hkl}\Sigma_i I_{hkl,i}$.

‡ FOM : figure of merit.

Table S3. Refinement statistics.

	Native	S-anomalous
Resolution (Å)	30–2.2	20–3.0
$R_{work}^{*}/R_{free}^{\dagger}$ (%)	20.64/22.87	20.30/24.47
No. atoms		
Protein	2,431	2,431
Heme	43	43
Ion/lipid	368	48
Water	32	0
B-factors (Å^2)		
Protein	55.30	48.58
Heme	41.72	37.98
Ion/lipid	82.70	66.14
Water	49.90	-
R.m.s. deviations		
Bond lengths (Å)	0.017	0.012
Bond angles (°)	2.01	1.30
Ramachandran plot		
Favored (%)	96.74	95.77
Allowed (%)	2.93	3.90
Outlier (%)	0.33	0.33
PDB-ID	6A2J	6IED

* $R_{work} = \Sigma_{hkl}||F_{obs}|-|F_{calc}||/\Sigma_{hkl}|F_{obs}|$.
† R_{free} was calculated by using 5% of the reflections that were not included in the refinement as a test set.

Additional data S1 (separate file)

The coordinate file for the structural model for the substrate-binding state (the PDB format).